

A Panoramic Fringe Projection system



V.H. Flores^{a,*}, L. Casaletto^b, K. Genovese^b, A. Martínez^a, A. Montes^a, J.A. Rayas^a

^a Centro de Investigaciones en Óptica, A.C., León, Gto., Mexico

^b School of Engineering, University of Basilicata, Potenza, Italy

ARTICLE INFO

Article history:

Received 15 August 2013

Received in revised form

11 December 2013

Accepted 11 February 2014

Available online 3 March 2014

Keywords:

Panoramic Fringe Projection

360°

Conical mirror

Axicon

ABSTRACT

In this work, we present a novel Panoramic Fringe Projection system (PFP) to retrieve the three-dimensional topography of quasi-cylindrical objects along their full length and around the entire circumference. The proposed procedure uses a 45° concave conical mirror to project a circular sinusoidal fringe pattern onto a specimen placed coaxially to the mirror, and at the same time, to image the modulated fringe pattern diffused from the object surface. In order to obtain the required sensitivity, an axicon is used to create a divergent fringe pattern with constant pitch. By processing the phase map, information on the radius over the full 360° surface of the sample is obtained. To verify the feasibility of the PFP measurement, a target sample with known shape-discontinuities has been tested. The proposed method demonstrated to be able to retrieve the full topography of complex shaped samples for a large variety of applications in the industrial and biomedical fields.

© 2014 Elsevier Ltd. All rights reserved.

1. Introduction

Fringe Projection (FP) is a well-known high-resolution non-contact technique used to retrieve the 3D topography of an object in a wide range of applications in industry, medicine, reverse engineering, etc. [see [1,2] and reference therein]. Among others, an application of particular interest is to reconstruct the object surface along its entire length and around its full 360° circumference, i.e. to perform a ‘whole-body’ measurement. This task is commonly accomplished by using either a single fixed FP system to sequentially capture different portions of the object (e.g. adopting a turntable arrangement) or multiple FP systems to perform measurement simultaneously from different viewpoints [3]. The entire object surface is then obtained by merging overlapping measured point clouds from the different views in an unique global coordinate system. This merging procedure is particularly critical and can affect the overall accuracy of the measurement.

In this paper we present a novel Panoramic Fringe Projection (PFP) system to retrieve simultaneously the 360° shape of quasi-axial-symmetrical objects from a single viewpoint by using a conical mirror and a conical lens. In literature conical mirrors have been already used for a large variety of radial-metrology applications such as for measuring deformation of cylinders on the inner and outer surfaces with Ligtienberg moiré [4] and white light interferometry [5], respectively, for performing inner profile

measurement with a ring-shaped laser beam [6] and for retrieving both shape and deformation of complex shaped objects with Video Dimension Analyzer [7] and Panoramic-Digital Image Correlation [8] systems.

In this work, the conical mirror is used to transform the single camera view into a panoramic view, and, together with the axicon, to project the fringe pattern over the 360° lateral surface of the object with a given angle at a constant pitch. The paper first describes the rationale behind the measurement and the experimental set-up, then presents and discuss the feasibility and performance of the proposed technique by performing a shape measurement on a quasi-axial-symmetrical target object with two longitudinal slots.

2. Panoramic fringe projection (PFP)

The Panoramic fringe projection system here presented has been developed starting from the most common FP scheme in which a commercial liquid crystal display (LCD) projector is used to project a computer-generated sinusoidal fringe pattern on the surface of interest imaged by a camera. If the projector is positioned at a given angle θ with respect to the viewing direction, the fringe pattern is distorted by the shape of the object and, in the special case of collimated projection and observation from infinity, it is possible to relate the height $h(x, y)$ of a given point $P(x, y, z)$ of the object surface with respect to a reference plane (usually the $x-y$ plane, i.e. $h = z$)

* Corresponding author. Tel.: +52 477 1397244.

E-mail addresses: viktor@cio.mx, viktorhfm@gmail.com (V.H. Flores).

and the phase $\phi(x, y)$ through Eq. (1)

$$h(x, y) = \frac{\phi(x, y)}{2\pi} \times \frac{p}{\sin \theta} \quad (1)$$

where p is the period of the sinusoidal fringe pattern [see e.g. scheme of standard FP system in Ref. [2]].

To commute a standard FP measurement to a Panoramic FP system, either projection and observation need to be transposed from a Cartesian-coordinate system to a cylindrical-coordinate system. To realize a 360° view of the lateral surface of a quasi-symmetrical sample similarly as reported in [5,7,8], a concave 45° conical mirror can be positioned coaxial to a single camera by making use of a beam-splitter as sketched in Fig. 1a. In this figure, a video projector is also positioned coaxially to the camera and to the conical mirror and it is used to project a sinusoidal circular pattern that is reflected on the lateral surface of the object (here a cylinder) placed inside the cone. Although the system depicted in Fig. 1a possesses either a panoramic projection and observation, it would be not able to measure the shape of the sample since $\theta = 0$, i.e. the system has no sensitivity. To introduce an angle $\theta \neq 0$ between the projection and viewing directions, a convex axicon [9,10] is here used to create a divergent conical fringe pattern with a constant pitch (i.e. with a constant sensitivity) according to the scheme sketched in Fig. 1b.

Fig. 2 shows a close-view picture of the experimental set-up used in this study to obtain the optical scheme depicted in Fig. 1b. To obtain a bright collimated source of light, a slides projector was disassembled and its 240 W high performance lamp was mounted separately similarly to the scheme reported in [11]. In particular, an IR reflector and a heat absorber is used to reject the heat produced by the lamp, then the light is condensed and collimated and hence used to illuminate a transmissive Spatial Light Modulator (SLM) with a 800×600 pixel² resolution (32 μm^2 pixel size) to create the sinusoidal circular fringe pattern to project onto the sample. A couple of polarizers placed before and after the SLM allows to use it in the amplitude modulation mode. Just after the second polarizer, an axicon (50 mm diameter and 130° aperture) transforms the collimated circular pattern in a conical (divergent) pattern of concentric circles of constant pitch. The light passes through a 45° beam-splitter and hits the concave surface of the conical mirror that reflects it back on the lateral surface of the sample with an angle $\theta \approx 14^\circ$ with respect to the viewing direction. Finally the fringe pattern on the lateral surface of the sample is imaged through the beam splitter from a 1280×1024 pixel² 8-bit B/W CCD camera equipped with a 7000 macro NAVITAR telecentric zoom objective (18–108 mm focal length).

3. PFP data processing

Fig. 3 reports the image formation scheme of a typical PFP measurement with the virtual camera and the virtual projector separated by an angular distance θ . Here, the position of a point P on the object surface (in this case a cylinder) can be expressed in the Cartesian-coordinate system x, y, z (with z axis coincident with the cone axis and the origin in the cone vertex, see Fig. 3) as $P(x_p, y_p, z_p)$, (mm, mm, mm) and in a cylindrical coordinate system as $P(\alpha_p, r_p, z_p)$, (rad, mm, mm). The point P is imaged in $P_i(u_p, v_p)$, (pixel, pixel) and $P_i(\beta_p, \rho_p)$, (rad, pixel) in a 2D Cartesian and in a polar-coordinate system of the camera sensor, respectively (with the origin of the polar system located in the image centre $C(u_c, v_c)$, (pixel, pixel)). If the system is correctly aligned and viewing from infinity is obtained (by using a telecentric lens), $\alpha_p = \beta_p$ and $\rho_p = MF \times z_p$ where MF (pixel/mm) is the magnification factor of the camera lens. The cylinder in the figure is the analogous of the reference plane for a standard FP system. In fact, the projected

circular fringe pattern remains unaltered when projected onto a nominally perfect cylindrical sample ($r = \text{constant}$) placed coaxial to the conical mirror. Analogously to standard FP, when a sample with a $r = f(\alpha, z)$ is placed in place of the cylinder, the observed fringe pattern is distorted since PFP is sensitive along the radial direction, i.e. it measures the departure of the radius of the sample from the radius of the reference cylinder. Analogously to Eq. (1), the relation between Δr and $\Delta\phi$ for PFP can be written as:

$$\Delta r(\alpha, z) = k \times \Delta\phi(\beta, \rho) \quad (2)$$

where k is a constant that it is a function of the geometry of the system and that can be evaluated through calibration [2].

In this work, the full-field phase map of the reference cylinder and of the sample has been calculated with the Four-Frames Phase Shifting (PS) algorithm [12,13]. The PS technique makes use of multiple fringe patterns with a phase shifts between successive frames. Accordingly, the registered sinusoidal fringe pattern intensity I_n of the n th frame can be written as [1]

$$I_n(\beta, \rho) = a(\beta, \rho) + b(\beta, \rho) \cos [\phi(\beta, \rho) + (n-1)\delta] \quad \forall n \in [1, N] \quad (3)$$

where $a(\beta, \rho)$ is the background intensity, $b(\beta, \rho)$ is the fringe amplitude, $\phi(\beta, \rho)$ is the phase and δ is the phase step. For the Four-Frames PS algorithm, $\delta = \frac{\pi}{2}$ and $N=4$. In this work, the wrapped phase distribution has been calculated by solving for $\phi(\beta, \rho)$ the system of Eq. (3) and then unwrapping it with an algorithm that uses a system of iso-phase contours for better dealing with the circular fringe pattern [14].

4. PFP experiments and results

To prove the feasibility of the proposed PFP system and the validity of the developed data processing routines, a series of tests has been performed on (i) a highly accurate cylinder (2.490 ± 0.005 mm diameter), (ii) a step-wise sample (with three different radii of 2–4 mm) and (iii) a quasi-axial-symmetrical sample with two longitudinal slots. These three tests served to (i) obtain the reference phase map, (ii) calibrate the system (i.e. calculating the k coefficient of Eq. (2)), (iii) obtain the phase map of a generally shaped object.

Before running the test, the system has been aligned by using a laser line (for the projection unit) and the Direct Linear Transformation method [15] for the camera. In particular, a dot-calibration pattern glued on the outward 30° conical portion of the conical mirror (see Fig. 3 and [8,15] for details) allowed to retrieve the intrinsic parameters (and hence the MF of the lens) and the extrinsic parameters of the camera (to locate the camera with respect to the x, y, z coordinate system). The relative position of camera and the conical mirror was adjusted by acting on the gimbal mount of the mirror and the multiaxial stage where the camera was fixed until a satisfactory alignment of the axes of camera and the conical mirror was reached.

Fig. 4 shows the image data related to the measurement on the sample pictured in Fig. 5a. In particular, from Fig. 4a to d, it is possible to see the result of transforming the four original images (Fig. 4a) into a single wrapped phase map (Fig. 4b), then unwrapping it (Fig. 4c) and finally obtaining the $\Delta\phi(\beta, \rho)$ distribution (Fig. 4d) by subtracting the unwrapped phase map with the analogous phase distribution of the reference cylinder (not reported). The $\Delta r(\alpha, z)$ distribution was obtained by multiplying the $\Delta\phi(\beta, \rho)$ distribution for the coefficient $k=1.57$ mm/rad obtained from calibration. The z coordinate of the measured point was obtained by dividing ρ for the magnification factor MF .

Fig. 5b and c show the results of the PFP measurement in terms of radius and error on radius with respect to the theoretical radius (5.8 mm external diameter, 3 mm internal diameter) for the sample in Fig. 5b. The PFP system and data processing procedure was able

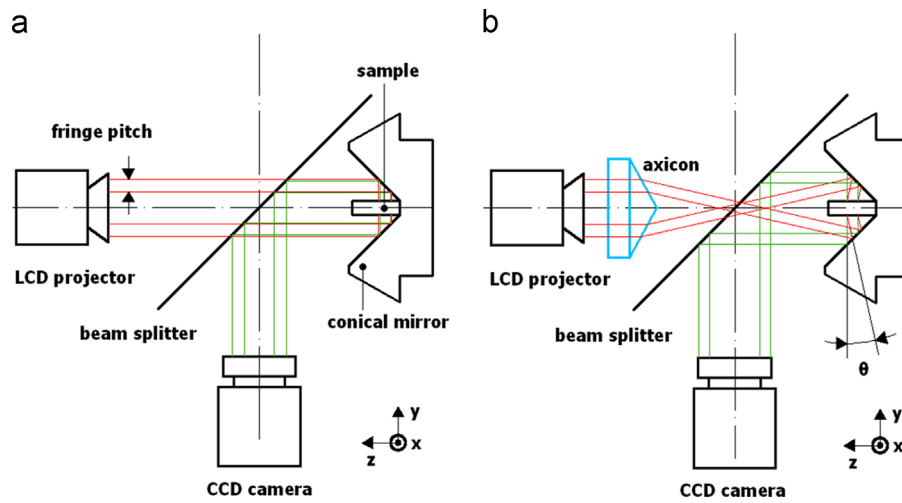


Fig. 1. Rationale of the PFP technique: (a) the set-up without the axicon; (b) the set-up with the axicon. Red rays indicate the projected pattern, green rays indicate the observed pattern. (For interpretation of the references to color in this figure legend, the reader is referred to the web version of this article.)

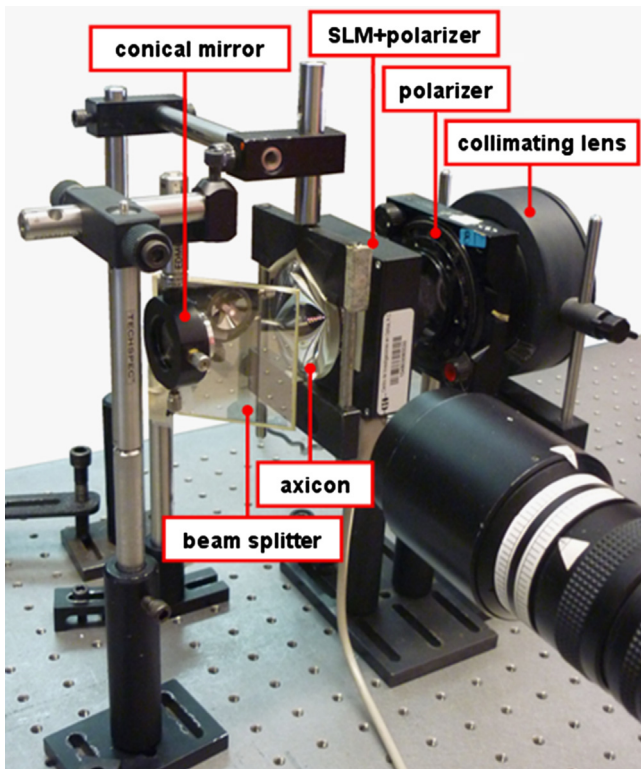


Fig. 2. Partial close-view of the experimental set-up.

to correctly measure the shape of the sample though with poor resolution due to the low sensitivity (small θ angle between projection and observation directions). Error on radius (calculated as $err_r = abs(r_{nom} - r_{cal})$ between nominal and calculated radius) is 0.11 ± 0.08 mm.

5. Concluding remarks

In this paper we presented a novel Panoramic Fringe Projection system able to reconstruct the full 360° shape of an object by using a conical mirror and a conical lens to realize a panoramic observation and projection, respectively. With respect to other FP applications to

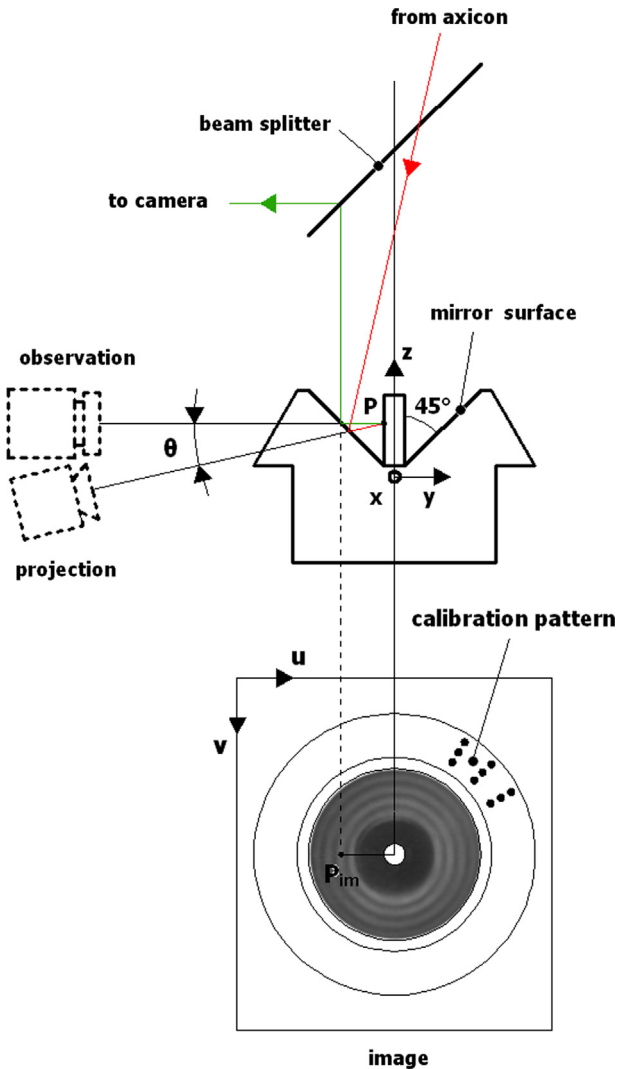


Fig. 3. Scheme for PFP data reduction.

whole-body measurements, the main strength point of the proposed method is the capability to capture the entire surface of the sample with a single camera from a single viewpoint, thus avoiding time

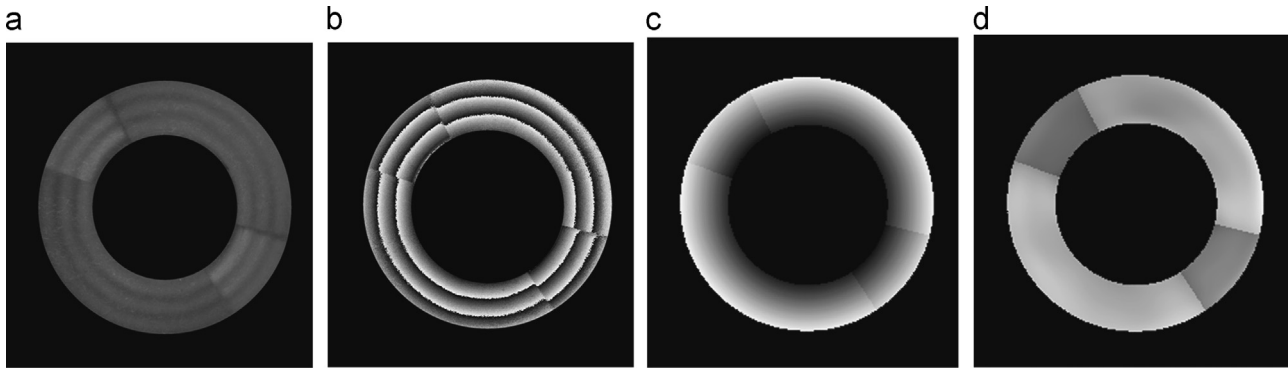


Fig. 4. Image sequence of fringe pattern analysis: (a) original masked image; (b) phase map; (c) unwrapped phase map; (d) phase difference between object and reference.

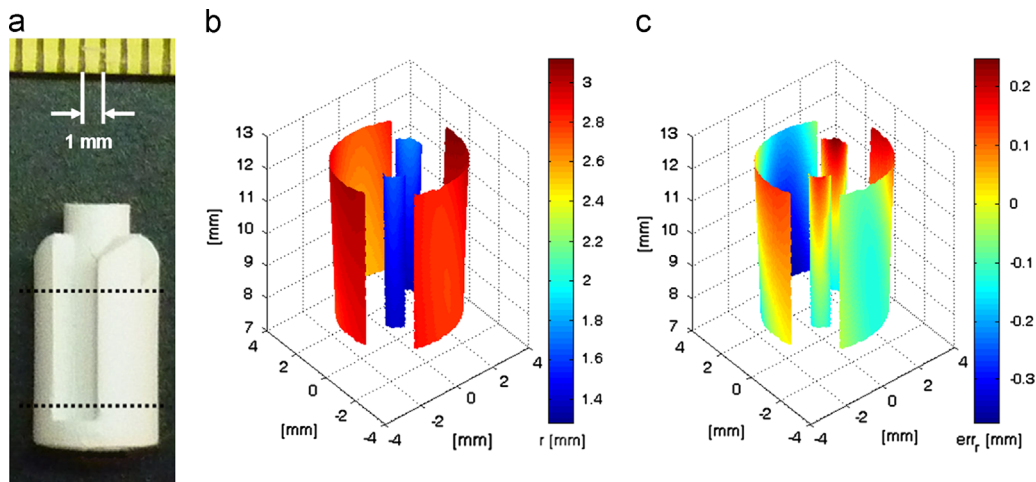


Fig. 5. Results of PFP topography measurement of the object in panel (a): (b) plot of radius and (c) plot of error on radius.

consuming merging procedures that could decrease the accuracy of the measurement. Here, a Four Frames PS algorithm has been used to retrieve the phase map of the object, however, if spatial PS algorithms are used [2], a single shot would be sufficient, i.e. time-resolved measurement could be performed. Moreover, imaging the lateral surface of a sample through a conical mirror increases the spatial resolution of one order of magnitude thus allowing to perform measurement on small-sized samples with ordinary off-the-shelf lenses [10,16].

The main limitation of the technique is the fact that the sensitivity of the measurement is strictly related to the axicon geometry that cannot be arbitrarily changed due to geometrical constraints in the relative positioning of the components. The results of this pilot study are however encouraging since the error in shape reconstruction is relatively low (about 5% on radius) notwithstanding a small sized sample was tested, no-high quality optics were used and any kind of correction of the non-sinusoidal projected and registered fringe patterns were applied. In view of the arguments above, we can conclude that further development of the proposed PFP method could be promising for either biomedical [16] and industrial applications, such as for reverse engineering of free form surfaces and online quality control.

Acknowledgements

This research is part of a bilateral project N. 146523 between Mexico and Italy, sponsored by CONACYT-MAE, and the project N.

180449, sponsored by CONACYT. V.H. Flores wants to thank CONACYT for his grant support.

References

- [1] AA VV. Special Issue on "Fringe Projection". *Opt Lasers Eng* 2010;48:133–256.
- [2] Gorthi SS, Rastogi P. Fringe projection techniques: whither we are? *Opt Lasers Eng* 2010;48(2):133–40.
- [3] Chen F, Brown GM, Song M. Overview of three-dimensional shape measurement using optical methods. *Opt Eng* 2000;39(1):10–22.
- [4] Krishnakumar S, Foster CG. Whole-field optical examination of cylindrical shell deformation. *Exp Mech* 1989;29(3):16–22.
- [5] Albertazzi A, Viotti MR, Miggiorini RM, Dal Pont A. Applications of a white light interferometer for wear measurement of cylinders. *Proc SPIE* 2008;7064(706408):1–10.
- [6] Yoshizawa, T, Wakayama, T. Development of an inner profile measurement instrument using a ring beam device. In: *Proceedings of SPIE 7855, optical metrology and inspection for industrial applications, 78550B* (2010).
- [7] Genovese K. A video-optical system for time-resolved whole-body measurement on vascular segments. *Opt Lasers Eng* 2009;47:995–1008.
- [8] Genovese K, Lee YU, Humphrey JD. Novel optical system for in vitro quantification of full surface strain fields in small arteries: I. Theory and design. *Comput Meth Biomech Biomed Eng* 2011;14(3):213–25.
- [9] Dépret B, Verkerk P, Hennequin D. Characterization and modeling of the hollow beam produced by a real conical lens. *Opt Commun* 2002;211(1–6):31–8.
- [10] Wei MD, Shiao WL, Lin YT. Adjustable generation of bottle and hollow beams using an axicon. *Opt Commun* 2005;248:7–14.
- [11] Bothe T, Osten W, Gesierich A, Jüptner W. Compact 3D camera. *Proc SPIE* 2002;4778:48–59.
- [12] Creath K. Phase-measurement interferometry. In: Wolf E, editor. *Progress in optics, vol. 5*. Amsterdam: North-Holland; 1988. p. 349–93.
- [13] Servin M, Estrada JC, Quiroga JA. The general theory of phase shifting algorithms. *Opt Express* 2009;17(24):21867–81.

- [14] Estrada JC, Vargas J, Flores JM, Quiroga A. Windowed phase unwrapping using a first-order dynamic system following iso-phase contours. *Appl Opt* 2012;51(31):7549–53.
- [15] Abdel-Aziz YI, Karara HM. Direct linear transformation from comparator coordinates into object space coordinates in close range photogrammetry. In: *Proceedings of the ASP/UI symposium on close-range photogrammetry*, Urbana, Illinois; 1971. p. 1–8.
- 16 Genovese K, Lee YU, Lee AY, Humphrey JD. An improved panoramic digital image correlation method for vascular strain analysis and material characterization. *J Mech Behav Biomed Mater*, Special issue on 'Inverse Problems' 2013;27:132–42.

ID	Title	Pages
743500	A Panoramic Fringe Projection system	5

Related Articles



<http://fulltext.study/journal/717>



-  **Categorized Journals**
Thousands of scientific journals broken down into different categories to simplify your search
-  **Full-Text Access**
The full-text version of all the articles are available for you to purchase at the lowest price
-  **Free Downloadable Articles**
In each journal some of the articles are available to download for free
-  **Free PDF Preview**
A preview of the first 2 pages of each article is available for you to download for free

<http://FullText.Study>